INSTITUTE OF PHYSICS PUBLISHING JOURNAL OF PHYSICS: CONDENSED MATTER

J. Phys.: Condens. Matter **17** (2005) 399–411 doi:10.1088/0953-8984/17/3/001

Density anomaly in a competing interactions lattice gas model

Alan B de Oliveira and Marcia C Barbosa[1]

Instituto de Física, Universidade Federal do Rio Grande do Sul, Caixa Postal 15051, 91501-970, Porto Alegre, RS, Brazil

E-mail: barbosa@if.ufrgs.br

Received 7 September 2004, in final form 30 November 2004
Published 7 January 2005
Online at stacks.iop.org/JPhysCM/17/399

Abstract

Water and other tetrahedral liquids are characterized by a density anomaly whose origin is not well understood. A very simple model of a short-range attraction followed by an outer shell repulsion is proposed as a test potential for the density anomaly. We show that these competing interactions when applied to a two-dimensional lattice gas leads to the formation of two liquid phases and to the appearance of a density anomaly. The coexistence line between the two liquid phases meets a critical line between the fluid and the low-density liquid phase at a tricritical point. The line of maximum density emerges in the vicinity of the tricritical point, close to the demixing transition.

1. Introduction

Water is an anomalous substance in many respects. Most liquids contract upon cooling. This is not the case for water, a liquid where the specific volume at ambient pressure starts to increase when it is cooled below $T = 4\,^{\circ}\mathrm{C}$ [1]. Besides, in a certain range of pressures, water also exhibits an anomalous increase of compressibility and specific heat upon cooling [2–4]. It is less well known that water diffuses faster under pressure at very high densities and at very low temperatures [5] and that the viscosity of water decreases upon increasing pressure [6–8].

It was proposed a few years ago that these anomalies are related to a second critical point between two liquid phases, a low-density liquid (LDL) and a high-density liquid (HDL) [9]. This critical point, discovered by computer simulations, might be located at the supercooled region beyond the line of homogeneous nucleation and thus cannot be experimentally measured. This hypothesis has been supported by indirect experimental results [7, 10]. In spite of the limit of 235 K below which water cannot be found in the liquid phase without crystallization, two amorphous phases were observed at much lower temperatures [11]. There is evidence, although yet under test, that these two amorphous phases are related to two liquid phases in fluid water [12, 13].

[1] Author to whom any correspondence should be addressed.

0953-8984/05/030399+13$30.00

Water is not an isolated case. There are also other examples of tetrahedrally bonded molecular liquids such as phosphorus [14, 15] and amorphous silica [16] that also are good candidates for having two liquid phases. Moreover, other materials such as liquid metals [17] and graphite [18] also exhibit thermodynamic anomalies. Unfortunately a coherent and general interpretation of the low-density liquid and high-density liquid phases is still missing. The relation between liquid polymorphism and density anomaly has been a subject of debate in recent theoretical literature [19].

What type of potential would be appropriate for describing the tetrahedrally bonded molecular liquids? Directional interactions are certainly an important ingredient in obtaining quantitative predictions for network-forming liquids like water [20, 21]. However, the models that are obtained from this approach are too complicated. Isotropic models became the simplest framework to understand the physics of the liquid–liquid phase transition and liquid state anomalies.

Recently it has been shown that the presence of two liquid phases can be associated with a potential with an attractive part and two characteristic short-range repulsive distances. The smaller of these two distances is associated with the hard core of the molecule, and the larger one with the soft core [19]. Acknowledging that core-softened (CS) potentials may engender a demixing transition between two liquids of different densities, a number of CS potentials were proposed to model the anisotropic systems described above. The first suggestion was made many years ago by Stell and co-workers in order to explain the isostructural solid–solid transition ending in a critical point [22, 23]. Debenedetti *et al*, using general thermodynamic arguments, confirmed that CS potentials can lead to a coefficient of thermal expansion negative and consequently to a density anomaly [24]. This, together with the increase of the thermal compressibility, has been used as indications of the presence of two liquid phases [25, 26] which may be hidden beyond the homogeneous nucleation. The difficulty with these approaches is that continuous potentials usually lead to crystallization at the region where the critical point would be expected. Consequently, the analysis of the presence of both the two liquid phases and the critical point becomes indirect.

Despite the apparent success of the introduction of CS potentials, it is not clear that the presence of two liquid phases and a density anomaly are due to the short-range shoulder [24] or if they result from the existence of two competing scales.

In this work we analyse another type of model system where two competing scales are also present. We study a potential with a hard core, a short-range attractive part and a repulsive shell. While the attraction accounts both for the van der Waals and hydrogen bonding interactions, the outer shell repulsion introduces the orientational order present in the hydrogen bonds. Therefore, the two scales emerge as a result of the competition between a first-neighbour attraction and second-neighbour repulsion.

In order to circumvent crystallization that appears in the continuous potentials, we work in a two-dimensional lattice gas. We show that this very simple system exhibits both a density anomaly and two liquid phases. However, instead of having a critical point ending the coexistence line between the two liquid phases, it has a tricritical point as the locus where the critical line meets the first-order coexistence line between the two liquid phases.

The paper goes as follows. In section 2 the model is presented, the mean field analysis is given in section 3, results from simulations are discussed in section 4, and our findings are summarized in section 5.

2. The model

Our system is represented by a square lattice with N sites. Associated with each site there is an occupational variable, σ_i. If the site is occupied by a molecule, $\sigma_i = 1$, otherwise $\sigma_i = 0$. Each

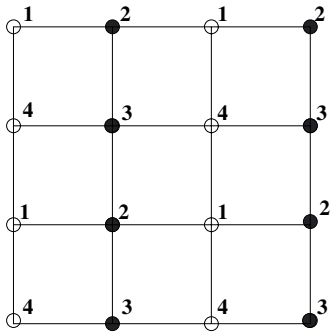

Figure 1. Sub-lattices.

site interacts with its nearest neighbours with attractive interactions and with its next-nearest neighbours with repulsive interactions. Therefore the Hamiltonian of this system is given by

$$\mathcal{H} = -V_1 \sum_{\langle ij \rangle} \sigma_i \sigma_j - V_2 \sum_{\langle\langle ik \rangle\rangle} \sigma_i \sigma_k - \mu \sum_i \sigma_i, \tag{1}$$

where the first sum is over the four nearest-neighbour sites and the second sum is over the four next-nearest-neighbour sites. The last term in equation (1) refers to the chemical potential contribution. Here we consider periodic boundary conditions.

In order to help the visualization of the phases that might be present in the system, the lattice is divided into four sub-lattices: 1, 2, 3, 4 (see the example in figure 1).

The sub-lattice density is given by

$$\rho_\beta = \frac{4}{N} \sum_{j \in \beta} \sigma_j, \qquad \beta = 1, \ldots, 4. \tag{2}$$

The ground state is obtained from the minimum value of Hamiltonian (equation (1)). For $V_1 > 0$ and $V_2 < 0$, the ground state has two possible scenarios: $V_1 < -2V_2$ and $V_1 > -2V_2$. In the first case and for high chemical potential, $\mu > -3V_1 - 4V_2$, all sites are occupied and the system is in the dense liquid (DL) phase. As the chemical potential is decreased some sites becomes empty and, at $\mu = -3V_1 - 4V_2$, there is a phase transition from the dense liquid phase to the structured dilute liquid (SDL) phase, illustrated in figure 1. On decreasing the chemical potential, at $\mu = -V_1$ there is a phase transition between the structured dilute liquid and the gas phase. If $V_1 > -2V_2$ and $\mu > -2V_1 - 2V_2$ the system is in the dense liquid phase and at $\mu = -2V_1 - 2V_2$ it has a phase transition from the SDL to the gas phase.

3. Mean-field approximation

The mean-field analysis follows the sub-lattice strategy introduced by Binder [27]. Even though it does not takes fluctuations into account, this approach gives an overview of the phase diagram that is quite helpful for making the right parameters choice for simulations. Moreover, Binder's method is able to capture the phase transition that other mean-field schemes miss. The approach goes as follows. The chemical potential acting on the system is rewritten as the sum of four potentials, one for each sub-lattice, namely:

$$\mu = \tfrac{1}{4} \sum_{\alpha=1}^{4} \mu_\alpha. \tag{3}$$

The use of independent chemical potentials may be necessary in a more general problem, where each sub-lattice is composed of a different type of molecule. For our model we have $\mu = \mu_\alpha, \alpha = 1, 2, 3, 4$. Now, rewriting the Hamiltonian, equation (1), in terms of the sub-lattices, we get the following expression:

$$\mathcal{H} = -\sum_{\alpha=1}^{4}\sum_{i\in\alpha} H_\alpha^{\text{eff}}(\{\sigma_j\})\sigma_i, \tag{4}$$

where

$$H_\alpha^{\text{eff}}(\{\sigma_j\}) = \mu_\alpha + \sum_{\beta=1}^{4}\sum_{i\in\beta} J_{ij}\sigma_j, \qquad i \in \alpha$$

and where the relations between J_{ij}, V_1 and V_2 are given by $J_{12} = J_{21} = J_{23} = J_{32} = J_{34} = J_{43} = J_{14} = J_{41} = V_1$ and $J_{13} = J_{31} = J_{24} = J_{42} = V_2$. The mean-field approximation here consists of replacing H_α^{eff} by its mean value, which leads to

$$\langle H_\alpha^{\text{eff}}\rangle = \mu_\alpha + \sum_{\beta=1}^{\nu}\epsilon_{\alpha\beta}\rho_\beta, \qquad i \in \alpha, \quad j \in \beta, \tag{5}$$

where $\rho_\beta = \langle\sigma_j\rangle$ and

$$\epsilon_{\alpha\beta} = \sum_{i(\neq j)} J_{ij}, \qquad i \in \alpha, \quad j \in \beta.$$

Substituting equation (5) in (4) we obtain

$$\mathcal{H}^{\text{MF}} = -\sum_{\alpha=1}^{4}\sum_{i\in\alpha}\left(\sum_{\beta=1}^{4}\epsilon_{\alpha\beta}\rho_\beta + \mu_\alpha\right)\sigma_i + \frac{1}{2}\sum_{\alpha=1}^{4}\frac{N}{4}\sum_{\beta=1}^{4}\epsilon_{\alpha\beta}\rho_\beta\rho_\alpha, \tag{6}$$

where the last term corrects for overcounting. Equation (6) is the Hamiltonian in the mean-field approximation which leads to the grand potential per site given by

$$\begin{aligned}\phi^{\text{MF}} = {} & -k_{\text{B}}T\ln 2 - \frac{k_{\text{B}}T}{4}\sum_{\alpha=1}^{4}\ln\cosh\left[\frac{1}{2k_{\text{B}}T}\left(\sum_{\beta=1}^{4}\epsilon_{\alpha\beta}\rho_\beta + \mu_\alpha\right)\right] \\ & - \tfrac{1}{8}\sum_{\alpha=1}^{4}\left(\sum_{\beta=1}^{4}\epsilon_{\alpha\beta}\rho_\beta + \mu_\alpha\right) + \tfrac{1}{8}\sum_{\alpha=1}^{4}\sum_{\beta=1}^{4}\epsilon_{\alpha\beta}\rho_\alpha\rho_\beta,\end{aligned} \tag{7}$$

where k_{B} is the Boltzmann factor and T is the temperature.

The density of each sub-lattice, derived from the grand potential, is given by

$$\begin{aligned}\rho_\alpha &= -4\left(\frac{\partial\phi^{\text{MF}}}{\partial\mu_\alpha}\right)_{T,\mu_{\alpha\neq\beta}}, \qquad \alpha = 1, 2, 3, 4, \\ &= \frac{1}{2} + \frac{1}{2}\tanh\left[\frac{1}{2k_{\text{B}}T}\left(\sum_{\beta=1}^{4}\epsilon_{\alpha\beta}\rho_\beta + \mu_\alpha\right)\right].\end{aligned} \tag{8}$$

The phase diagram illustrated in figure 2 was obtained by solving equation (8) for fixed values of temperature and chemical potential. For simplicity, we assume that $V_1 = 1$ and $V_2 = -1$. At high temperatures, each sub-lattice is half full in an disorganized way that characterizes the fluid phase. As the temperature is lowered at a fixed chemical potential, $\mu^* \equiv \mu/V_1 > 1$, the system goes from the fluid to the dense liquid phase continuously and no phase transition is observed. Similarly, at very low chemical potentials, $\mu^* < -1$, as the temperature is decreased, the system goes from the fluid to the gas phase continuously with

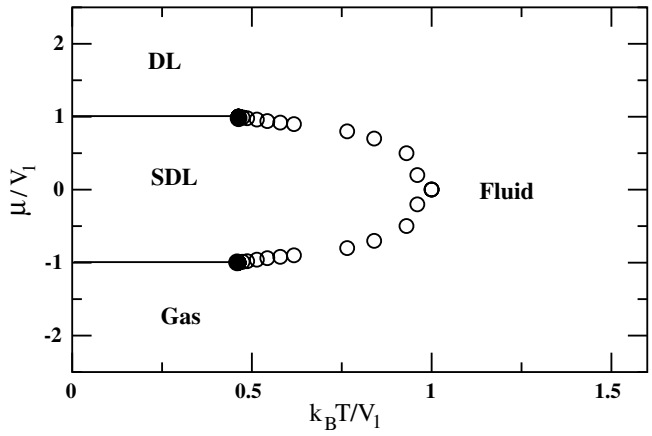

Figure 2. Mean-field phase diagram: the open circles represent the second-order phase transition, the solid lines are the two first-order phase transitions and the two filled circles are the two tricritical points.

no phase transition. For intermediate chemical potentials, $-1 > \mu^* > 1$, at $T = T_c$ there is a continuous phase transition between the fluid phase and the structured dilute liquid phase. The coexistence line between the gas phase and the structured diluted liquid meets this continuous phase transition at a tricritical point. Another similar point is observed at the contact between the SDL–DL coexistence line and the critical line. The density is monotonic, therefore no density anomaly is observed.

4. Monte Carlo simulations

The rather simple mean-field approach introduced in the previous section is unable to account for the density anomaly. Therefore, Monte Carlo simulations in grand canonical ensemble were performed. The Metropolis algorithm[2] was used to study a square $L \times L$ lattice and $|V_2|/V_1 = 1$. Different system sizes $L = 10, 20, 30, 40, 50$ were investigated. The typical equilibration time was 1500 000 Monte Carlo time steps for each lattice site.

The non-zero temperature phase diagram was obtained as follows. For a fixed temperature and chemical potential the density of each sub-lattice and the specific heat was computed by averaging over 5000 measures. Between consecutive measures, τ Monte Carlo steps were performed to decorrelate the system. The *correlation time* τ was calculated using the density correlation function [28]:

$$\chi(t) = \frac{1}{t_{\max} - t} \sum_{\tilde{t}=0}^{t_{\max}-t} \rho(\tilde{t})\rho(\tilde{t}+t) - \left[\frac{1}{t_{\max} - t} \sum_{\tilde{t}=0}^{t_{\max}-t} \rho(\tilde{t})\right]\left[\frac{1}{t_{\max} - t} \sum_{\tilde{t}=0}^{t_{\max}-t} \rho(\tilde{t}+t)\right]. \qquad (9)$$

Figure 3 shows the total density for the lattice sizes $L = 50, 40, 30, 20$ and 10, from top to bottom (see also inset) and for fixed chemical potential $\mu^* = 0.5$. According to this graph, one could conclude that no phase transition happens as the temperature is decreased at a fixed chemical potential $\mu^* = 0.5$. However, analysing the sub-lattice's densities illustrated in figures 4–7 (here we are illustrating only the result obtained for $L = 20$), it is clear from the density fluctuations at $T^* = T/V_1 = 0.45$ that a phase transition must be present. The peak in the specific heat shown in figure 8 confirms the existence of this transition and helps to determine the exact location of the critical point at T_c^*.

[2] Our system is quite simple and does not require the use of a more sophisticated Monte Carlo algorithm.

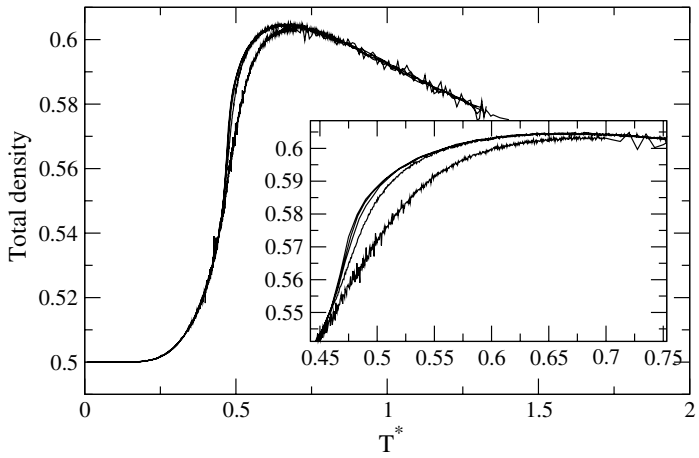

Figure 3. Total density for the 50, 40, 30, 20 and 10 lattices, from top to bottom.

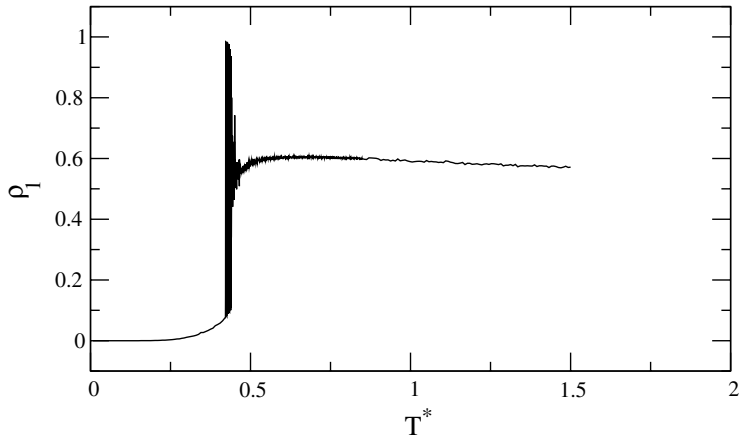

Figure 4. Sub-lattice 1.

The energy histograms constructed for fixed temperatures around the critical temperature T_c^* are shown in figures 9–11. For temperatures above and below T_c^*, there is only one peak, indicating that the transition is continuous (two peaks would be a signature of a first-order transition).

Analyzing again figures 4–7 it can be seen that for $T^* > T_c^* = 0.45$ the sub-lattice densities $\rho_\beta \approx 0.56$, indicating that the system is in the fluid phase, while for $T^* < 0.45$, $\rho_1 = \rho_2 = 0$ and $\rho_3 = \rho_4 = 1$, which is a signature of a structured dilute liquid. Hence, at $T_c^* = 0.45$ there is a continuous transition between the fluid and the SDL phases. The error bars associated with the location of the critical temperatures for the lattice sizes $L = 10, 20$ are respectively $\Delta T = 4 \times 10^{-4}$ and $\Delta T = 7.5 \times 10^{-3}$, while for the lattice sizes $L = 30, 40, 50$ they are $\Delta T = 6.5 \times 10^{-3}$.

Criticality happens only at the thermodynamic limit. Therefore, in order to determine the actual critical temperature, it is necessary to extrapolate the results obtained for the finite systems to $L \to \infty$. The critical temperatures for the finite systems were obtained from the

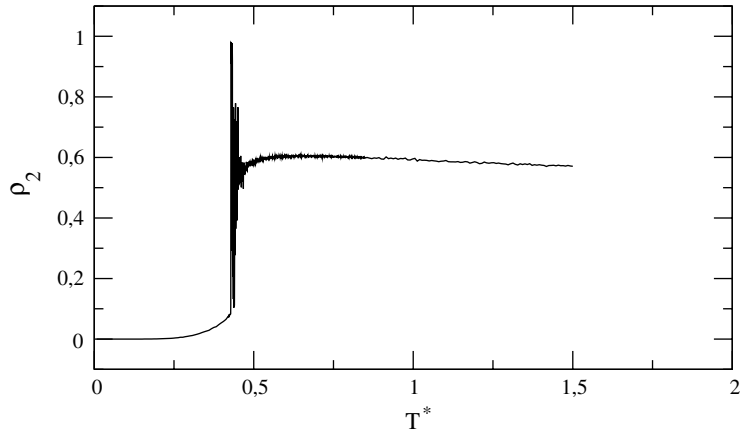

Figure 5. Sub-lattice 2.

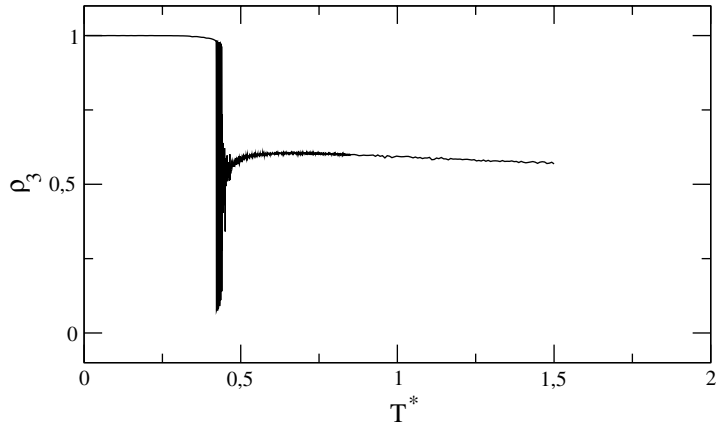

Figure 6. Sub-lattice 3.

maximum of the specific heat and from the minimum of the fourth-order Binder's cumulant V_E [29]. This last method requires computing, for each lattice size, the quantity

$$V_E = 1 - \frac{\langle E^4 \rangle}{3\langle E^2 \rangle^2}, \tag{10}$$

where E is the total energy of the system.

Figure 12 shows the critical temperatures for different lattice sizes and fixed chemical potential, $\mu^* = 0.5$, obtained from the specific heat and from the minimum of the Binder's fourth-order cumulant. The critical temperature for the infinite system becomes $T_c^* = 0.466$ when derived from the specific heat and $T_c^* = 0.467$ from Binder's cumulant. The difference between these two results is smaller than the error bars of both numbers. The lattice $L = 10$ was excluded from the extrapolation because it is so far from the infinite size limit that its inclusion would require including nonlinear terms in the extrapolation.

Figure 3 shows that for a fixed chemical potential the density has a maximum at a certain temperature $T_{\max}$. The temperature of maximum density as a function of the chemical potential is illustrated in figure 13.

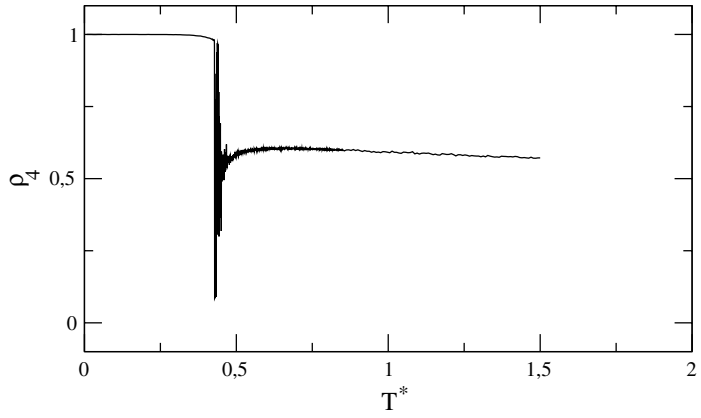

Figure 7. Sub-lattice 4.

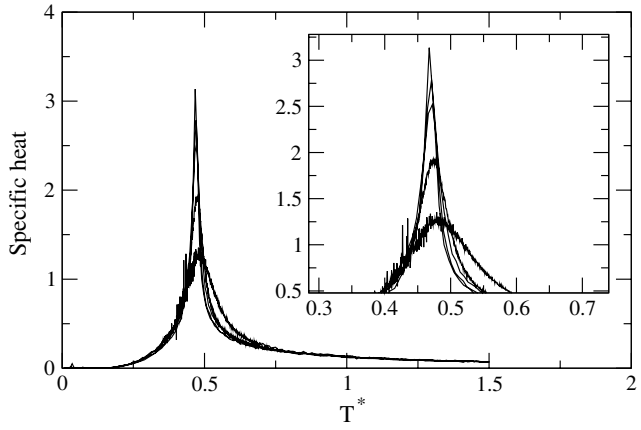

Figure 8. Specific heat for $\mu^* = 0.50$ and $L = 50, 40, 30, 20, 10$ from top to bottom.

In order to observe the first-order phase transitions between the gas and SDL phases and between the SDL phase and the DL phase, simulations at fixed temperature and varying chemical potential were performed. Figure 14 shows that for $T^* = 0.19$ the transition between the SDL phase and the DL phase happens at $\mu^* = 1$. At low chemical potentials a similar transition is observed between the gas and the SDL phases. At the intersection between the critical line and the first-order phase transition lines two tricritical points appear.

The pressure was computed by numerical integration of the Gibbs–Duhem equation, $S\,\mathrm{d}T - V\,\mathrm{d}P + N\,\mathrm{d}\mu = 0$, at fixed temperature. Integration was carried out from effective zero density, at which the pressure is zero, to obtain $P(\rho, T)$ isotherms. The pressure isotherms show that an inversion of the behaviour of the density as a function of temperature takes place at intermediate pressures, in the SDL phase. The phase diagrams for other values of $V_1 < -2V_2$ are similar to the one we present here. In the case of $V_1 > -2V_2$ both the two liquid phases and the density anomaly are not present.

5. Conclusions

From a microscopic point of view, water anomalies have been interpreted qualitatively, since the work of Bernal [30], in terms of the presence of an extensive hydrogen bond network

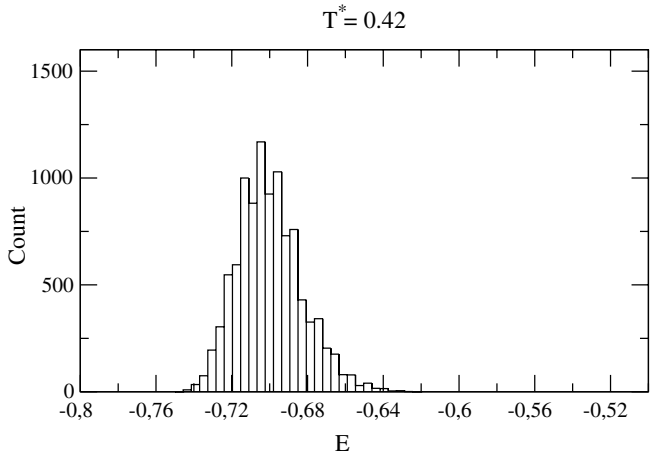

Figure 9. Energy histogram for $T < T_c$, $\mu^* = 0.50$ and $L = 20$.

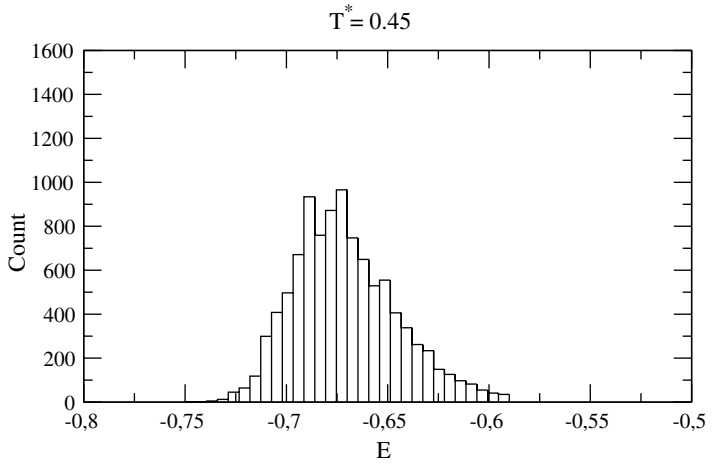

Figure 10. Energy histogram for $T \approx T_c$, $\mu^* = 0.50$ and $L = 20$.

which persists in the fluid phase [31]. In the case of lattice models, the main strategy has been to associate the hydrogen bond disorder with bond Potts states [20, 21]. The coexistence between two liquid phases follows from the presence of an order–disorder transition, and a density anomaly is introduced ad hoc by the addition to the free energy of a volume term proportional to a Potts order parameter.

In this work we propose a description also based on occupational degrees of freedom, but the orientational degrees of freedom are in the competition between nearest and next-nearest interactions. Inclusion of the competing interactions aims to represent in an effective way the directionality of the hydrogen bonding that favours open structures. With our approach, the density anomaly arises naturally with no need of the addition of a volume term to the free energy.

For testing our assumption that having two competing scales leads to a demixing transition and thermodynamic anomalies, we studied a very simple system: a two-dimensional lattice gas with competing interactions and in contact with reservoirs of particles and temperature.

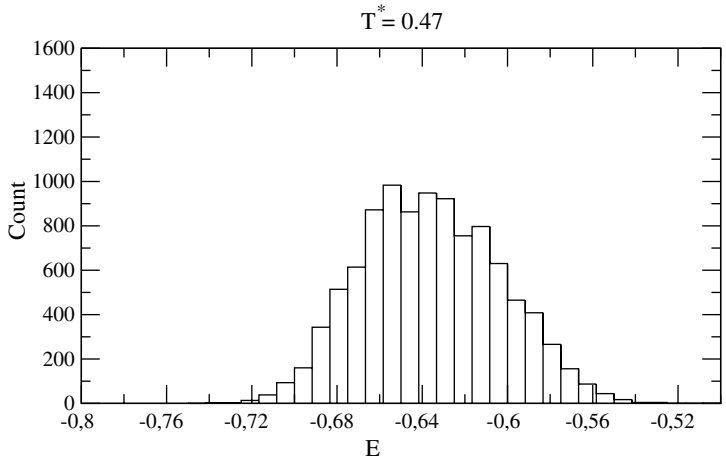

Figure 11. Energy histogram for $T > T_c$, $\mu^* = 0.50$ and $L = 20$.

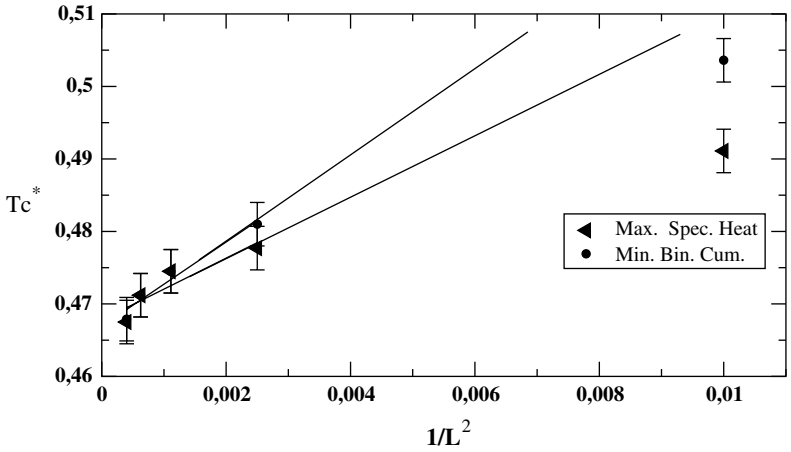

Figure 12. $T_c^* \times 1/L^2$ for $L = 10, 20, 30, 40, 50$. The circles are the minimum of Binder's cumulant and the triangles are the maximum of the specific heat.

Extending our calculations to three dimensions will just increase the computational cost without bringing any new physics to the problem. Competing interactions models exhibit qualitatively similar phase diagrams in two and three dimensions.

Our system exhibits two liquid phases and a line of density anomalies. Differently from the general belief, the density anomaly line is not associated with a single critical point [9] but with a line of critical points. Moreover, the density anomaly does not arise from a softened core potential but from an outer shell repulsion that competes with a short-range attraction. We believe that the common ingredient that leads to the presence of demixing between two liquid phases both in softened core potentials and in the present model is the existence of two competing scales for the interaction [33, 32].

The relation between the form of the potential, criticality and the density anomaly goes as follows. While the short-range attraction favours the formation of a dense liquid phase, the outer shell repulsion favours the formation of an open structure, the SDL phase. In systems

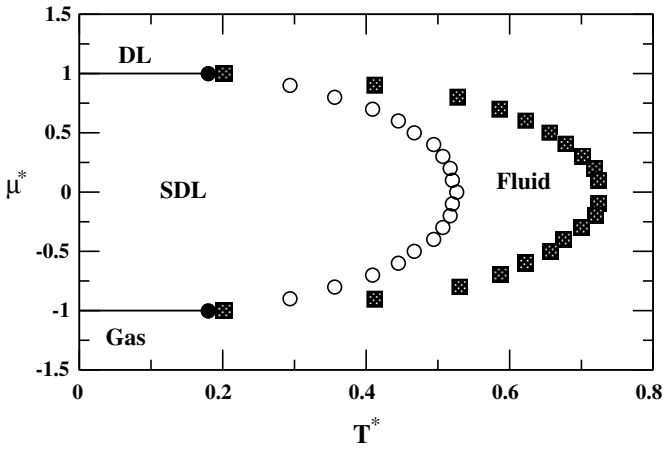

Figure 13. $\mu^* \times T^*$ phase diagram: the circles indicates the critical line, the solid lines show the first-order transitions, the squares locate the temperature of maximum density and the full circles are the tricritical points. The error bars are smaller than the symbols.

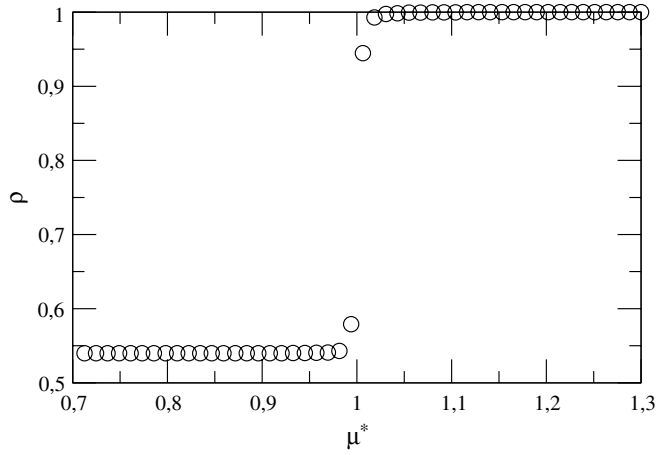

Figure 14. $\rho \times \mu^*$ for $T^* = 0.19$.

dominated by short-range attractive forces, if the pressure is kept fixed, the density increases on cooling. In our case, similar behaviour is only observed at high temperatures where short-range interactions are dominant. As the temperature is decreased, the outer shell repulsion prevents the density increasing beyond a certain limit. Therefore, the same competition responsible for the appearance of two liquid phases leads to the density anomaly.

One should point out that the presence of a critical line instead of a single critical point as one could generally expect [9] is not surprising. Due to the lattice structure, the SDL phase is not one single phase but the region where two different phases coexist (empty/full rows and empty/full columns). These two phases become critical together with the DL phase at the tricritical point that is also the locus where the critical line ends.

In summary, we have shown that both a density anomaly and multicriticality can arise from a very simple interaction model. Obviously our results are just qualitative and cannot be quantitatively applied to water or to other anomalous liquids.

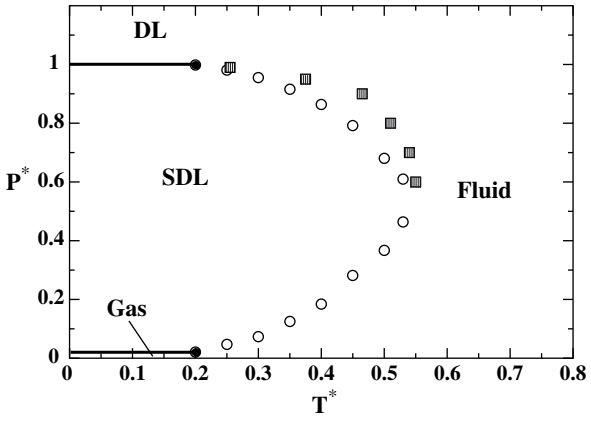

Figure 15. $p^* \equiv p/|V_1| \times T^*$ phase diagram: the solid lines indicate first-order transitions, the empty circles locate the continuous line, the squares show the temperature of maximum density and the filled circles are the tricritical points. The error bars are smaller than the symbols.

Acknowledgments

This work was supported by the Brazilian science agencies CNPq, FINEP, Capes and Fapergs.

References

[1] Waller R 1964 *Essays of Natural Experiments* (New York: Johnson Reprint Corporation)
[2] Prielmeier F X, Lang E W, Speedy R J and Lüdemann H-D 1987 *Phys. Rev. Lett.* **59** 1128
[3] Prielmeier F X, Lang E W, Speedy R J, Lüdemann H-D and Bunsenges B 1988 *Phys. Chem.* **92** 1111
[4] Haar L, Gallagher J S and Kell G S 1984 NBS/NRC Steam Tables *Thermodynamic and Transport Properties and Computer Programs for Vapor and Liquid States of Water in SI Units* (Washington, DC: Hemisphere) pp 271–6
[5] Netz P A, Starr F W, Stanley H E and Barbosa M C 2001 *J. Chem. Phys.* **115** 344
[6] Debenedetti P G 1996 *Metastable Liquid* (Princeton, NJ: Princeton University Press)
[7] Mishima O and Stanley H E 1998 *Nature* **396** 329
[8] Yoshimura Y and Bunsenges B 1991 *Phys. Chem.* **95** 135
[9] Poole P H, Sciortino F, Essmann U and Stanley H E 1992 *Nature* **360** 324
Poole P H, Sciortino F, Essmann U and Stanley H E 1993 *Phys. Rev.* E **48** 3799
Sciortino F, Poole P H, Essmann U and Stanley H E 1997 *Phys. Rev.* E **55** 727
Harrington S, Zhang R, Poole P H, Sciortino F and Stanley H E 1997 *Phys. Rev. Lett.* **78** 2409
[10] Speedy R J and Angell C A 1976 *J. Chem. Phys.* **65** 851
[11] Mishima O, Calvert L D and Whalley E 1984 *Nature* **310** 393
[12] Smith R S and Kay B D 1999 *Nature* **398** 788
[13] Mishima O and Suzuki Y 2002 *Nature* **419** 599
Martonak R, Donadio D and Parrinello M 2004 *Phys. Rev. Lett.* **92** 225702
[14] Katayama Y, Mizutani T, Utsumi W, Shimomura O, Yamakata M and Funakoshi K 2000 *Nature* **403** 170
[15] Monaco G, Falconi S, Crichton W A and Mezouar M 2003 *Phys. Rev. Lett.* **90** 255701
[16] Lacks D J 2000 *Phys. Rev. Lett.* **84** 4629
[17] Cummings P T and Stell G 1981 *Mol. Phys.* **43** 1267
[18] Togaya M 1997 *Phys. Rev. Lett.* **79** 2474
[19] Franzese G, Malescio G, Skibinsky A, Buldyrev S V and Stanley H E 2001 *Nature* **409** 692
[20] Sastry S, Debenedetti P G, Sciortino F and Stanley H E 1996 *Phys. Rev.* E **53** 6144
[21] Franzese G, Marques M I and Stanley H E 2003 *Phys. Rev.* E **67** 011103
Franzese G and Stanley H E 2002 *J. Phys.: Condens. Matter* **14** 2201
[22] Hemmer P C and Stell G 1970 *Phys. Rev. Lett.* **24** 1284
Stell G and Hemmer P C 1972 *J. Chem. Phys.* **56** 4274

[23] Hoye J S and Hemer P C 1973 *Phys. Nor.* **7** 1
[24] Debenedetti P G, Raghavan V S and Borick S S 1991 *J. Phys. Chem.* **95** 4540
[25] Sadr-Lahijany M R, Scala A, Buldyrev S V and Stanley H E 1998 *Phys. Rev. Lett.* **81** 4895
[26] Scala A, Starr F W, La Nave E, Stanley H E and Sciortino F 2000 *Phys. Rev.* E **62** 8016
[27] Binder K and Landau D P 1980 *Phys. Rev.* B **21** 1941
[28] Newman M E J and Barkem G T 1999 *Monte Carlo Methods in Statistical Physics* (Oxford: Clarendon)
[29] Tsai S-H and Salinas S R 1998 *Braz. J. Phys.* **28** 58
[30] Bernal J D and Fowler R H 1933 *J. Chem. Phys.* **1** 515
[31] Tests of the cooperativity of the net are still being tested, e.g. Errington J R, Debenedetti P G and Torquato S 2002 *Phys. Rev. Lett.* **89** 215503
[32] Henriques V B and Barbosa M C 2004 Liquid polymorphism and density anomaly in a lattice gas model, submitted
[33] Balladares A L and Barbosa M C 2004 Density anomaly in core-softened lattice gas *J. Phys.: Condens. Matter* **16** 8811